Taylor & Francis
Taylor & Francis Group

Journal of Macromolecular Science, Part A
Pure and Applied Chemistry

ISSN: 1060-1325 (Print) 1520-5738 (Online) Journal homepage: https://www.tandfonline.com/loi/lmsa20

Electrospun Polyacrylic Acid Polymer Fibers Functionalized with Metallophthalocyanines for Photosensitizing and Gas Sensing Applications

Ruphino Zugle & Tebello Nyokong

To cite this article: Ruphino Zugle & Tebello Nyokong (2012) Electrospun Polyacrylic Acid Polymer Fibers Functionalized with Metallophthalocyanines for Photosensitizing and Gas Sensing Applications, Journal of Macromolecular Science, Part A, 49:4, 279-287, DOI: 10.1080/10601325.2012.662006

To link to this article: https://doi.org/10.1080/10601325.2012.662006

Journal of Macromolecular Science, Part A: Pure and Applied Chemistry (2012) **49**, 279–287

ISSN: 1060-1325 print / 1520-5738 online
DOI: 10.1080/10601325.2012.662006

Taylor & Francis
Taylor & Francis Group

Electrospun Polyacrylic Acid Polymer Fibers Functionalized with Metallophthalocyanines for Photosensitizing and Gas Sensing Applications

RUPHINO ZUGLE and TEBELLO NYOKONG*

Department of Chemistry, Rhodes University, Grahamstown, South Africa

Received October 2011, Accepted November 2011

The photophysical and photochemical properties of tetraaminophthalocyanine complexes of lutetium and zinc covalently linked to polyacrylic acid were studied alongside those of unsubstituted zinc phthalocyanine within the same polymeric fiber matrix. All three phthalocyanines within the solid fiber matrices showed photoactivity by the generation of singlet oxygen as was observed in solution. The fluorescence behaviors of the composite fibers equally parallel those in solution. For the unsubstituted zinc phthalocyanine composite, the fiber showed fluorescence quenching on interaction with gaseous nitrogen dioxide similar to that in DMF and, thus could be a promising nanofabric material in developing optoelectronic devices that are responsive to the gas.

Keywords: Lutetium tetraaminophthalocyanine, zinc phthalocyanine, polyacrylic acid, singlet oxygen, fluorescence

1 Introduction

Metallophthalocyanines have attracted a great deal of attention for quite some time for possible applications in various fields including color display technology, gas sensors and photodynamic therapy (1–5). Attaching phthalocyanines or porphyrins to polymer support offers many advantages which do not exist when phthalocyanines are used alone (6–8). They include cooperative reactions in polymer chains, separation of active sites, the possibility of specific binding of different substrates on active sites and increase in stability. Phthalocyanine-containing polymeric materials have been designed for a wide range of applications, such as photosensitization (8) and sensing (9), as well as in medicine for low-toxicity photodynamic bactericidal activity (10). However, the use of electrospun fibers containing phthalocyanines is still less researched (8).

Electrospinning is a promising technique for incorporation of functional molecules into solid polymer fiber supports. It is simple, convenient, reproducible, and a generally versatile technique for generating fibers with diameters that range from several micrometers to tens of nanometers (11). Incorporation of phthalocyanines into electrospun polymer fibers has been reported with the functionality of the phthalocyanine still maintained in the solid fiber core. (12, 13).

In this work, we wish to harness the merits of electrospinning alongside the numerous applications of phthalocyanines to generate functionalized fibers for multiple purposes. Immobilization of phthalocyanines on polymer supports through covalent attachment has been found to prevent leakage during applications (14). In this work, we therefore used phthalocyanine complexes containing an amino group for chemical linking to polyacrylic polymer containing carboxylic acid functionalities. The photosensitizing ability and fluorescence properties of tetraaminophthalocyanine complexes of zinc (ZnTAPc) and lutetium ((Ac)LuTAPc, Ac = acetate) covalently linked to polyacrylic acid (PAA) through an amide bond (giving PAA/ZnTAPc and PAA/(Ac)LuTAPc, respectively) are assessed. The aim is to assess if phthalocyanines in the composite fibers exhibit similar photophysical and photochemical properties to those in solution. These properties are compared with unsubstituted zinc phthalocyanine embedded in a similar polymer fiber without a chemical bond, represented as PAA/ZnPc. The choice of Lu as a central metal is based on its large size which encourages intersystem crossing of the singlet excited state of the metallophthalocyanine to the triplet state which could possibly lead to high singlet oxygen quantum yield; the latter is essential for photodynamic therapy.

*Address correspondence to: Tebello Nyokong, Department of Chemistry, Rhodes University, Grahamstown 6140, South Africa. Tel: + 27 46 6038260; Fax: + 27 46 6225109; E-mail: t.nyokong@ru.ac.za

2 Experimental

2.1 Materials

The following chemicals were purchased from SAARCHEM; quinoline, n-hexane, dimethylsulfoxide (DMSO), N,N-dimethylfomamide (DMF) and sodium sulphite nanohydrate ($Na_2S.9H_2O$). Zinc phthalocyanine (ZnPc), 1,8-diazabicyclo[5.4.0] undec-7-ene (DBU), dicyclohexylcarbodiimide (DCC) 99%, 1,3-diphenylisobenzofuran (DPBF), polyacrylic acid (PAA) (Mw = 450,000 g/mol), lutetium(III) acetate, deuterateds dimethylsulfoxide (DMSO-d_6), and metallic copper were from Sigma Aldrich and nitric acid from Merck. 4-Nitrophthalonitrile (1) was synthesized according to literature procedures (15). Zinc tetraaminophthalocyanine (ZnTAPc) was synthesized and characterized following literature procedure (16, 17). Column chromatography was performed on silica gel 60 (0.04–0.063 mm) and preparative thin layer chromatography was performed on silica gel 60 P F_{254}.

2.2 Equipment

Infrared (IR) spectra were recorded on a Perkin-Elmer Fourier transform–IR (100 FT-IR) spectrophotometer. UV-Vis absorption spectra were recorded on a Shimadzu UV-2550 spectrophotometer. ^{1}H-NMR spectra were recorded on a Bruker AMX600 MHz in deuterated DMSO. Microanalyses were performed using a Vario-Elementar Microcube ELIII. Mass spectral data were recorded on ABI Vogager De-STR Maldi TOF instrument using α-cyano-4-hydroxycinnamic acid as a matrix. Scanning electron microscope (SEM) images were obtained using a JOEL JSM 840 scanning electron microscope.

Irradiations for singlet oxygen studies were done using a General Electric Quartz lamp (300W), 600 nm glass (Schott) and water filters, to filter off ultra-violet and far infrared radiations, respectively. An interference filter 670 nm with bandwidth of 40 nm was placed in the light path just before cell containing the sample. A Bruker Vertex 70-Ram II Raman spectrometer (equipped with a 1064 nm Nd:YAG laser and a liquid nitrogen cooled germanium detector) were used to collect Raman data. The Raman spectral data for PAA/ LuTAPc, PAA/ZnTAPc and PAA were obtained from the electropun fibers.

X-ray powder diffraction (XRD) patterns were recorded on a Bruker D8 Discover equipped with a proportional counter, using Cu-K_α radiation (λ = 1.5405 Å, nickel filter). Data were collected in the range from $2\theta = 5^\circ$ to 70°, scanning at 1° min^{-1} with a filter time-constant of 2.5 s per step and a slit width of 6.0 mm. Samples were placed on a zero background silicon wafer slide. XRD data were treated using Eva (evaluation curve fitting) software. Baseline correction was performed on each diffraction pattern by subtracting a spline fitted to the curved background and the full-width at half-maximum values used in this study were obtained from the fitted curves.

Fluorescence excitation and emission spectra were recorded on a Varian Cary Eclipse spectrofluorimeter. The fluorescence images were taken with a DMLS fluorescence microscope. The excitation source was a high-voltage mercury lamp and light in the wavelength range of 550–730 nm.

2.3 Photophysical and Photochemical Parameters

2.3.1 *Triplet State Yields and Lifetimes*

Triplet quantum yields were determined for (Ac)LuTAPc and ZnTAPc in DMF using a comparative method (18), Equation 1, with ZnPc as the standard.

$$\Phi_T = \Phi_T^{Std} \frac{\Delta A_T \varepsilon_T^{Std}}{\Delta A_T^{Std} \varepsilon_T} \quad (1)$$

where ΔA_T and ΔA_T^{Std} are the changes in the triplet state absorbances of the samples ((Ac)LuTAPc and ZnTAPc) and the standard, respectively. ε_T and ε_T^{Std} are the triplet state molar extinction coefficients for the samples ((Ac)LuTAPc and ZnTAPc) and the standard, respectively. Φ_T^{Std} is the triplet quantum yield for the standard, ZnPc ($\Phi_T^{Std} = 0.58$ in DMF) (19). The triplet lifetimes were determined by exponential fitting of the kinetic curve using the program ORIGIN Pro 8.

2.3.2 *Fluorescence Quantum Yield*

Fluorescence quantum yield (Φ_F) of (Ac)LuTAPc was determined in DMF by the comparative method (20), Equation 2:

$$\Phi_F = \Phi_F^{Std} \frac{F A_{Std} n^2}{F_{Std} A n_{Std}^2} \quad (2)$$

where F and F_{Std} are the areas under the fluorescence emission curves of (Ac)LuTAPc and the standard, respectively. A and A_{Std} are the respective absorbances of the sample and standard at the excitation wavelength. The same solvent was used for the sample and standard. Unsubstituted ZnPc in DMF ($\Phi_F^{Std} = 0.30$) (21) was employed as the standard. Both the sample and standard were excited at the same wavelength of 612 nm and emission spectrum was recorded from 630 nm to 790 nm. The absorbances of the solutions at the excitation wavelength were about 0.05 to avoid any inner filter effects. The fluorescence quantum yield, $\Phi_F = 0.0043$ for ZnTAPc is known in DMF (22).

2.3.3 *Singlet Oxygen Quantum Yield*

A chemical method was also employed to determine the singlet oxygen quantum yield, Φ_Δ, of (Ac)LuTAPc and ZnTAPc in DMF. The comparative method was used with ZnPc ($\Phi_\Delta^{ZnPc} = 0.56$ in DMF) (23–25), as the standard and

DPBF as singlet oxygen quencher, using Equation 3.

$$\Phi_{\Delta} = \Phi_{\Delta}^{\mathrm{ZnPc}} \times \frac{R^{\mathrm{sample}}}{\mathrm{R}^{\mathrm{ZnPc}}} \times \frac{\mathrm{I}^{\mathrm{ZnPc}}}{\mathrm{I}^{\mathrm{Sample}}} \quad (3)$$

where $\Phi_{\Delta}^{\mathrm{ZnPc}}$ is the singlet oxygen quantum yield for the ZnPc standard, $\mathrm{R}^{\mathrm{sample}}$ and $\mathrm{R}^{\mathrm{ZnPc}}$ are the DPBF photobleaching rates in the presence of (Ac)LuTAPc or ZnTAPc and ZnPc standard, respectively, while $\mathrm{I}^{\mathrm{sample}}$ and $\mathrm{I}^{\mathrm{ZnPc}}$ are the respective rates of light absorption by (Ac)LuTAPc or ZnTAPc and ZnPc standard. The initial DPBF concentrations were kept the same for both the standard and the sample. Molar extinction coefficient ($\mathrm{dm^3\ mol^{-1}\ cm^{-1}}$) of DPBF at $\lambda = 417$ nm in DMF of $\varepsilon = 23{,}000$ (26) was employed. For the modified fibers, the photoactivity was demonstrated in hexane using DPBF as a singlet oxygen quencher. The modified fibers (PAA/LuTAPc), (PAA/ZnTAPc) and (PAA/ZnPc) were suspended in the solution containing DPBF and irradiated using the photolysis set-up described above.

2.4 Synthesis of (Ac)LuTAPc (Sch. 1)

(Ac)LuTAPc was synthesized using the procedure reported for other MTAPc complexes (17). A mixture of anhydrous lutetium (III) acetate (134 mg, 0.38 mmol) and 4-nitrophthalonitile (**1**, 131 mg, 0.76 mmol) in quinoline (2.5 mL) was refluxed for 7 h under nitrogen atmosphere using DBU as catalyst. After cooling, the crude product was precipitated with n-hexane, filtered and dried. The crude product was purified using column chromatography on silica gel with DMF as eluting solvent. The solvent was evaporated to give product **2**. Product **2** was then stirred in 250 ml aqueous solution containing 10 g $NaS.9H_20$ for 24 h. The solid product was separated in a centrifuge and treated with 500 mL of 1M HCl. The residue was separated and treated with 500 mL of 1M NaOH for 1 h, after which the solid product was separated in a centrifuge, washed several times with de-ionized water and dried in a vacuum. Yield 17% IR: 3327 $\mathrm{cm^{-1}}$ N-H stretching, 1623 $\mathrm{cm^{-1}}$ N-H bending mode, 2846 and 2927 $\mathrm{cm^{-1}}$ (C-H aromatic), 1570 $\mathrm{cm^{-1}}$ C=O, 1443, 1434, 1347 and 1307$\mathrm{cm^{-1}}$ C-N vibrations due to the phthalocyanine ring. UV-Vis (DMF): λmax/nm (log ε) 350 (3.81), 704 (4.55), Calcd. for $C_{34}H_{23}N_{12}O_2Lu$; C 50.63, H 2.87, N 20.81. Found C 50.91, H 3.00, N 21.04%; ^{1}H NMR (DMSO-d_6) δ,ppm: 2.12 (3H, s, acetate CH_3), 4.02 (8H, s, NH_2), 8.29 (4H, s, Ar-H), 8.20 (4H, d, Ar-H), 8.00 (4H, d, Ar-H). MS (MALDI-TOF) (m/z): Calcd. 807; Found 807 [M^+].

2.5. Preparation of Fibers

A solution of PAA was prepared by dissolving 0.2 g in 100 mL of DMF. Dicyclohexylcarbodimide (DCC), 0.5 g

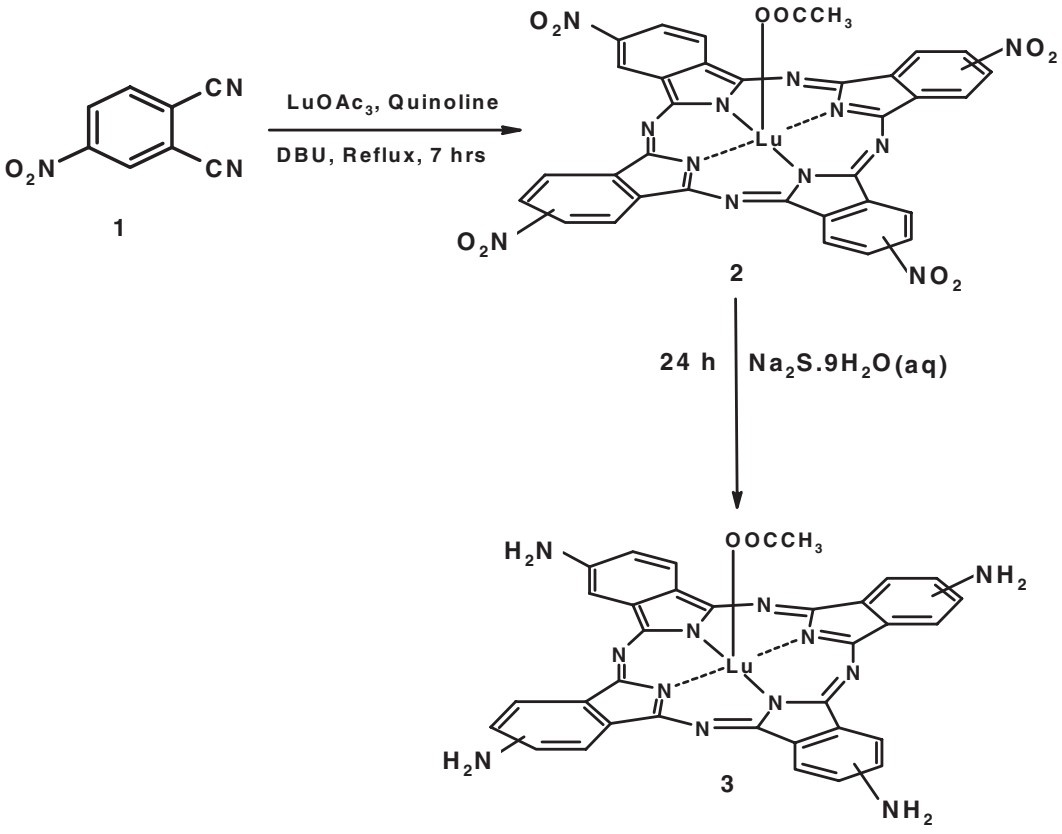

Sch. 1. Synthetic route for (Ac)LuTAPc. Ac = acetate.

was added and the solution stirred for four days. This is to activate the carbonyl of the carboxylic acid for covalent amide bond formation. A known mass (10 mg) of (Ac)LuTAPc or ZnTAPc was added to give a concentration of 1.24×10^{-4} M in the resulting solution. The mixture was stirred for several days while taking the IR spectra intermittently to monitor the amide bond formation, after which the composite was precipitated using diethyl ether and dried in a desiccator. For the conjugate of unsubstituted ZnPc with PAA, 10 mg (ZnPc) was mixed with 0.2 g (PAA) with no addition of DCC.

The solutions for electrospinning were prepared by dissolving 6.6 wt% of each composite in 1:4 (v/v) water/ethanol solvent mixture and stirred for 24 h. The following spinning conditions were used; 1 mL/h flow rate, 10 kV applied voltage and 15 cm collector distance. Similar conditions were used for PAA alone and PAA/ZnPc composite.

3 Results and Discussion

3.1 Characterization of ZnTAPc and (Ac)LuTAPc in Solution

3.1.1 *Spectroscopic Characterization*

ZnTAPc is well known (17, 23). The synthesis of (Ac)LuTAPc, is reported here for the first time and was characterized by ^{1}H-NMR, mass and IR spectroscopy, as well as elemental analysis. A molecular ion peak corresponding to [M^+] at 807 amu was obtained.

Infrared spectroscopic analysis of (Ac)LuTAPc showed a partially split peak around 3327 cm^{-1} which is characteristic of N-H stretching mode of a primary amine group (27). This is supported by the corresponding N-H bending mode at 1623 cm^{-1}. The C-H stretchings were observed at 2846 and 2927 cm^{-1}. The peak at 1590 cm^{-1} is attributed to C=O bond from the axial acetate group, while the C-N vibrations due to the phthalocyanine ring were observed at 1443, 1434, 1347 and 1307 cm^{-1}. The UV-visible spectral features of (Ac)LuTAPc and ZnTAPc in DMF are shown in Figure 1 with the broad Q-band characteristic of monomeric aminophthalocyanines. Table 1 shows that the Q band of ZnTAPc is more red-shifted than unsubstituted ZnPc due to the electron donating ability of amino groups. The Beer-Lambert law was obeyed for concentration below 1.42×10^{-5} M for (Ac)LuTAPc.

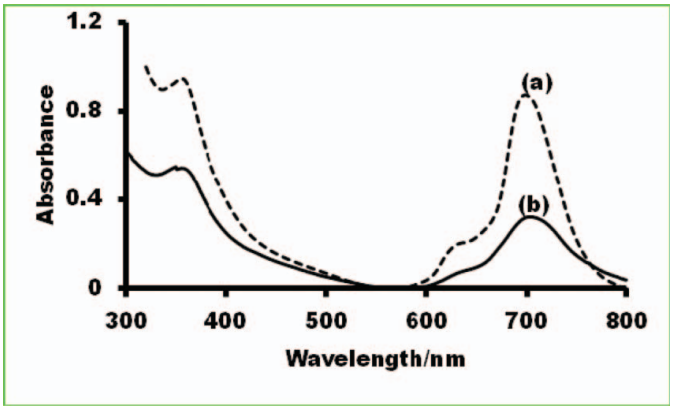

Fig. 1. UV-visible spectra of (a) 1×10^{-4} M ZnTAPc, (b) 1×10^{-5} M (Ac)LuTAPc in DMF. (Color figure available online).

3.1.2 *Photophysical and Photochemical Properties*

The fluorescence properties of (Ac)LuTAPc were studied in spectroscopic grade DMF. The phthalocyanine was found not to fluorescence at all. Low fluorescence of phthalocyanine complex of lutetium has been reported before (28) and is attributed to the heavy atom effect of the large diamagnetic lutetium metal which enhances intersystem crossing of the excited singlet state to the metastable triplet state. A similar explanation has also been suggested to explain the fluorescence behavior of phthalocyanine complex of hafnium, another large metal, which does not fluoresce at all (29). Therefore, fluorescence lifetime could not be measured for (Ac)LuTAPc. For the corresponding non-peripherally substituted ZnTAPc and peripherally tetra substituted ZnTAPc, very low Φ_F values (0.0011 and 0.0043 (Table 1), respectively) were obtained in DMF (23), due to the quenching effects of the amino group. The reported fluorescence lifetimes for ZnTAPc in Table 1 are similar to those of ZnPc. Thus, for (Ac)LuTAPc, which contains large central metal and in addition to the quenching effect of the amino group, the lack of fluorescence is not surprising.

The triplet quantum yield (Φ_T) refers to the fraction of absorbing photosensitizer molecules, which in their

Table 1. Photophysical and photochemical parameters for ZnPc, ZnTAPc and (Ac)LuTAPc in DMF. References in square brackets

Complex	λ_Q *(abs), nm*	λ_Q *(Emm), nm*	Φ_F	τ_F *(ns)*[a]	Φ_T	τ_T *(μs)*	Φ_Δ
ZnPc	670	681	0.30 [23]	3.69 ± 0.037 (100%) [23]	0.58 (19)	330 [25]	0.58 [25]
ZnTAPc	725	756	0.0043 [23]	2.49 ± 0.062(75%), 10.9 ± 2.33(25%) [23]	0.24	3.32	0.17
(Ac)LuTAPc	701	–	–	–	0.43	3.74	0.29

[a]Abundances in round brackets.

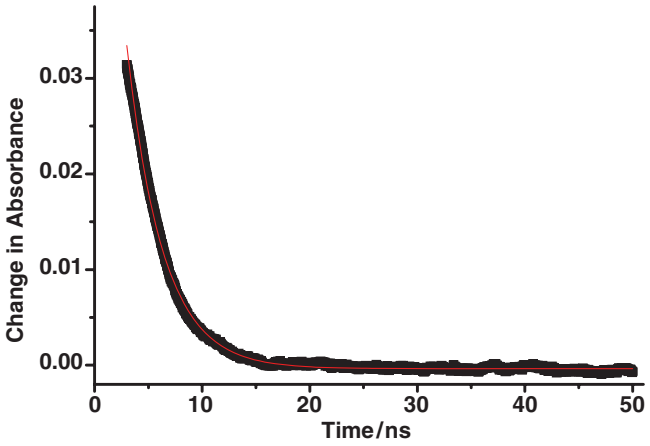

Fig. 2. Triplet decay curve of (Ac)LuTAPc in DMF at 490 nm: Excitation wavelength: 676 nm. (Color figure available online).

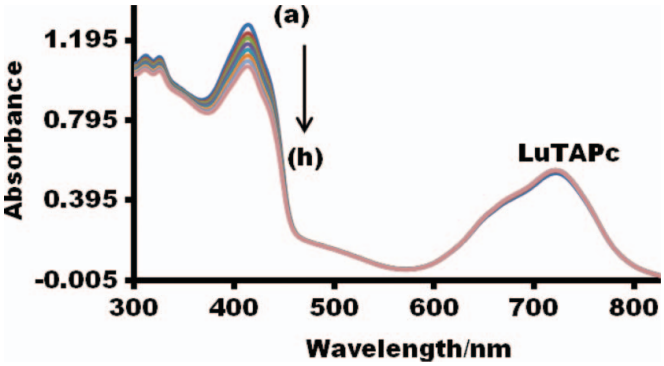

Fig. 3. Spectral changes during degradation of DPBF using (Ac)LuTAPc in DMF. Time interval: 5 sec. (Color figure available online).

singlet excited state, undergo intersystem crossing to the metastable triplet state. The triplet quantum yield for (Ac)LuTAPc in DMF was found to be 0.43 with a lifetime of 3.74 ± 0.01 μs. The triplet decay curve is shown Figure 2, which follows first order kinetics. For ZnTAPc, $\Phi_T = 0.24$ and triplet lifetime, $\tau_T = 3.32 \pm 0.01$ μs were obtained. For the corresponding non-peripherally substituted Zn$^{\alpha}$TAPc triplet-triplet absorption did not occur (23), due to the quenching of the first excited singlet state by the presence of amino group when located at the non-peripheral position, inhibiting the formation of its triplet state. At the peripheral position, the quenching induced by the amino group is not as pronounced and triplet absorption is observed with triplet yield of 0.24 and lifetime $\tau_T = 3.32 \pm 0.01$ μs as indicated in Table 1.

In this work, we investigated the possibility of (Ac)LuTAPc or ZnTAPc generating singlet oxygen by using a chemical method based on 1,3-diphenylisobenzofuran (DBPF), a singlet oxygen quencher in DMF. Unsubstituted ZnPc was used as standard. As shown in Figure 3, the band at 414 nm corresponding to DBPF, decreased in intensity on irradiation with visible light in the presence of (Ac)LuTAPc or ZnTAPc. This suggests generation of singlet oxygen by (Ac)LuTAPc or ZnTAPc in the presence of light. The singlet oxygen quantum yield (Φ_Δ) was determined by the comparative method to be 0.29 for (Ac)LuTAPc and 0.17 for ZnTAPc in DMF. The low Φ_Δ value for ZnTAPc corresponds to the lower values of its Φ_T compared to (Ac)LuTAPc, Table 1. The Φ_Δ values for both (Ac)LuTAPc and ZnTAPc are lower than for other ZnPc complexes (30).

3.2 Characterization of Fibers

3.2.1 *Microscopic Characterization*

Fiber diameter and morphology were assessed using the SEM technique. The fibers were generally cylindrical and unbranched with relatively wide diameter range (Fig. 4). In the case of non-functionalized PAA fibers, the diameters ranged from 124–930 nm, while the range for PAA/LuTAPc was 153–1356 nm and 130–1309 nm for ZnTAPc. The fibers of PAA had a number of beads. However, those of the functionalized ZnTAPc and (Ac)LuTAPc fibers had virtually no beads. This could be accounted for by the fact that phthalocyanines are high charge density aromatic macromolecules. Thus, their presence in the functionalized polymer solution will lead to an increase in charge density of the polymer solution. Such an increase in the net charge density of polymer solutions during electrospinning has been reported (31) to lead to elimination of beads similar to what has been observed in this work.

3.2.2. *Spectroscopic Characterization*

The conjugates were formed through an amide bond involving the NH_2 group of (Ac)LuTAPc and ZnTAPc with the carboxylic acid groups of PAA as illustrated in Scheme 2 for PAA/LuTAPc composite, while PAA/ZnPc was due to induced dipole-dipole interaction.

In this work, we established the covalent amide bond formation for (Ac)LuTAPc or ZnTAPc using FT-IR and Raman spectral techniques as discussed below.

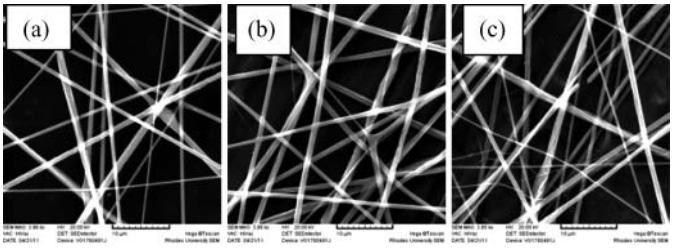

Fig. 4. Fiber mats of (a) PAA alone, (b) PAA/LuTAPc composite and, (c) PAA/ZnTAPc composite.

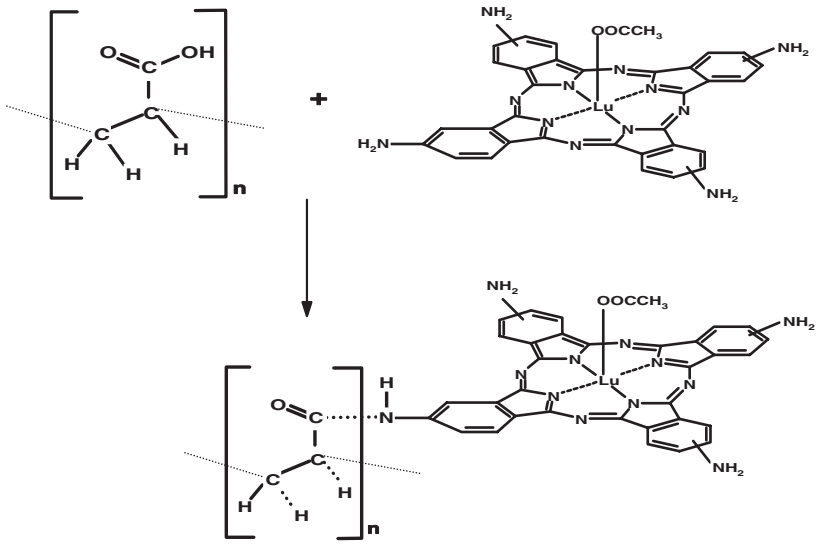

Sch. 2. Formation of amide bond between (Ac)LuTAPc and PAA.

3.2.2.1 FTIR spectra analysis. The FT-IR spectral features of polyacrylic acid (Fig. 5(a)), include the broad O-H band around 3100–3600 cm^{-1} and the carbonyl stretching at 1699 cm^{-1}. In the case of (Ac)LuTAPc (Fig. 5(b)), the partially split and broad band around 3270–3327 cm^{-1} may be assigned to asymmetric and symmetric stretching vibrations of the amino groups of the phthalocyanine (17). This is supported by the intense $–NH_2$ group in-plane bending vibration observed at 1623 cm^{-1}.

For PAA/LuTAPc composite (Fig. 5(c)), the N-H stretching vibration of the (Ac)LuTAPc has diminished in intensity, and the corresponding bending mode around 1623 cm^{-1} has almost disappeared. This suggests that the amino groups are engaged possibly in amide bond formation with PAA. The incomplete disappearance of these two bands due to the $–NH_2$ of the Pc could be due to the fact that not all four amino groups of any particular (Ac)LuTAPc molecule are engaged in the amide bond formation. There is a slight shift of the carbonyl position indicating electronic interactions between the components. Similarly, the position and intensity of the aromatic C-H of (Ac)LuTAPc as well as it characteristic phthalocyanine C-N vibrations, have their positions slightly shifted in the hybrid. These observations jointly suggest that the phthalocyanine molecules are bound within the polymer matrix through electronic interactions.

3.2.2.2 Raman spectra. The covalent linkage of (Ac)LuTAPc or ZnTAPc to PAA through amide bonds was further ascertained using Raman spectroscopy. Figure 6 shows the spectra of (a) PAA alone and (b) PAA/LuTAPc conjugate fiber. As shown in Figure 6(b), the peaks at 1606 cm^{-1} (I), 1445 cm^{-1} (II) and 1298 cm^{-1} which are low in intensities, are the characteristic amide peaks (32, 33). The appearance of these peaks further

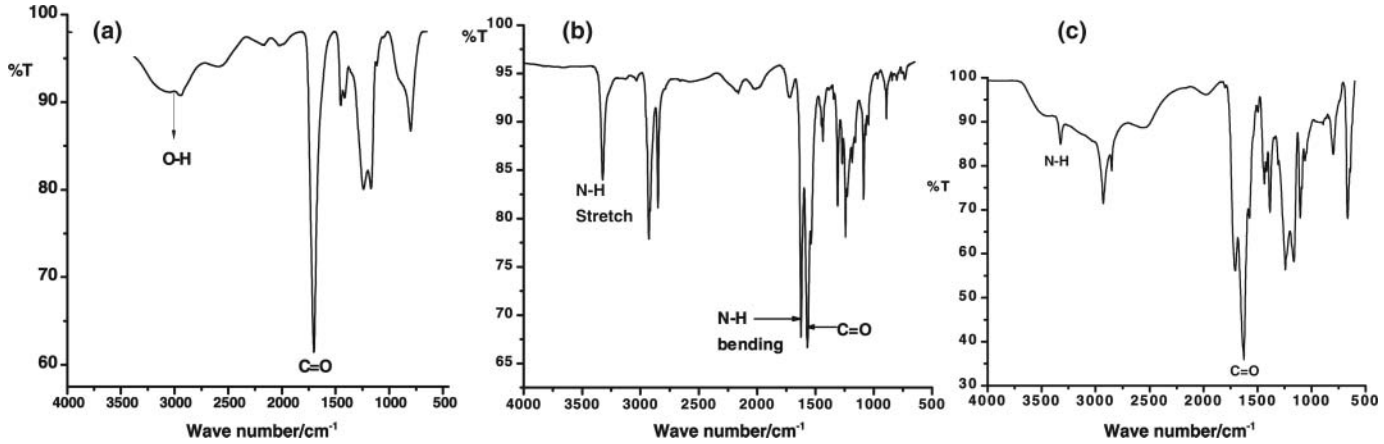

Fig. 5. FT-IR spectra of fibers (a) PAA, (b) (Ac)LuTAPc and, (c) PAA/LuTAPc hybrid.

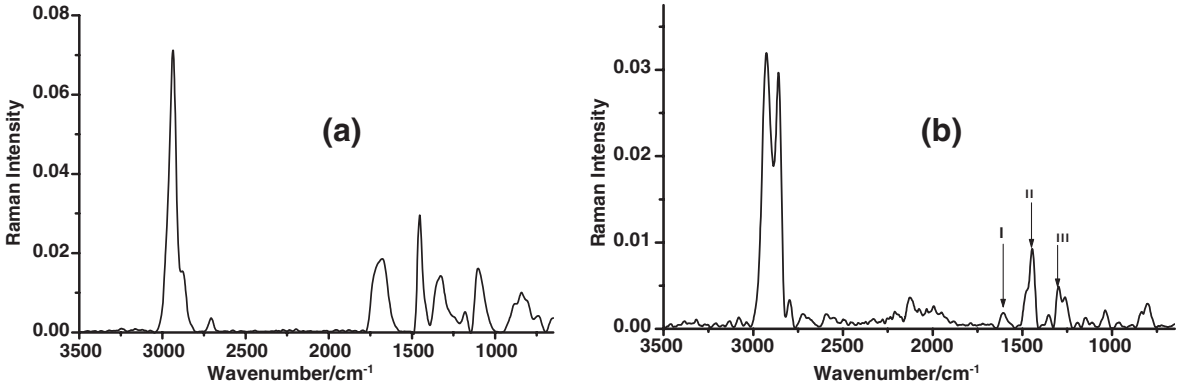

Fig. 6. Raman spectra of fibers (a) PAA and (b) PAA/LuTAPc.

confirms the attachment of (Ac)LuTAPc or ZnTAPc to PAA through covalent amide bond.

3.2.2.3 XRD patterns. The XRD pattern of (Ac)LuTAPc (Fig. 7(a)) shows a pronounced broad peak covering 2θ = 15–30° with maximum occurring around 24°. The broad nature of this peak indicates that phthalocyanine is amorphous. The peak maximum around 24° is close to the (002) reflection plane of carbon (34). In PAA alone, the XRD pattern, Figure 7(b) shows two broad peaks. In the conjugate there is an overlap of PAA peaks with those of (Ac)LuTAPc, Figure 7(c). The broadening in all peaks show the low crystallinity of (Ac)LuTAPc in the both pure form and within the polymer fiber.

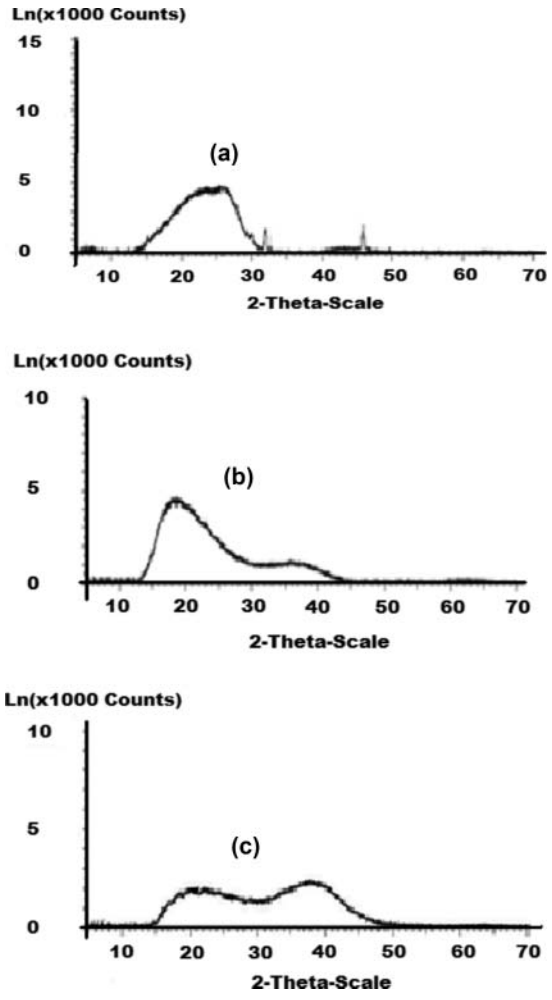

Fig. 7. X-ray diffraction patterns of (a) (Ac)LuTAPc powder, (b) PAA fiber and (c) PAA/LuTAPc fiber.

3.2.3 *Singlet Oxygen Generating Ability of Pcs in Functionalized Fibers*

The ability of the phthalocyanines ((Ac)LuTAPc, ZnTAPc and ZnPc) to generate singlet oxygen within the polymeric fiber matrices were assessed using DPBF as singlet oxygen quencher in hexane as solvent. In water, the fibers gradually dissolved to form gelatinous solution and as such water was not a suitable medium. Pieces of the functional fibers were placed in solutions of DBPF in hexane and irradiated using the setup as described above.

Figure 8 shows a typical degradation of DPBF when PAA/LuTAPc composite fiber was used. This demonstrates that the MPcs within the fiber matrix are still capable of generating singlet oxygen though a longer period of irradiation was required for a significant change of the absorbance of DPBF around 414 nm than in solution. This could be due to the fact that the inherent photophysical and photochemical behavior of the phthalocyanine can be altered when constrained within the environment of a polymeric matrix. Thus a

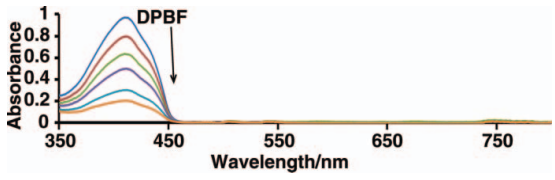

Fig. 8. Spectral changes during degradation of DPBF using PAA/LuTAPc composite fiber in hexane. Time interval: 15 min. (Color figure available online).

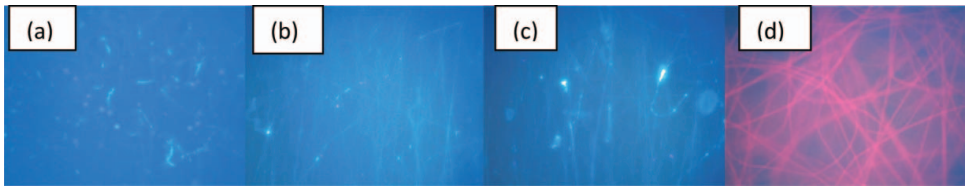

Fig. 9. Fluorescence micrographs of (a) ZnPc powder, (b) PAA/ZnTAPc fiber, (c) PAA/LuTAPc functionalized fiber, (d) PAA/ZnPc functionalized fiber. (Color figure available online).

direct correlation between the phthalocyanine behavior in solution and in solid fiber matrix cannot be feasible. Such an assertion has been put forward by Lang et al. (35). When PAA fiber alone was used, no degradation of DPBF occurred suggesting that the MPcs within the fibers are the agents involved in the singlet oxygen generation. The fact the MPcs showed photoactivity within the fiber matrix suggests that not all the MPcs molecules are completely encapsulated within the fiber but are found equally around the large exposed surface area of the fiber because of the smaller fiber diameters. The MPcs did not leach out of the fiber into solution as evidenced from the Q-band region of the sample solutions during photolysis. This confirms once again the bound nature of the MPcs within the fiber matrix.

3.2.4 *Fluorescence Microscopic Images*

The ability of the phthalocyanines ((Ac)LuTAPc, ZnTAPc and ZnPc) to fluoresce within the fiber matrix was investigated. The recorded fluorescence intensity images of the phthalocyanines within the fiber matrices are shown in Figure 9. The recorded intensity image of ZnPc emission in the fabric material is shown in Figure 9(d), which shows the uniformity in the emission intensity along all the fibers suggesting homogeneous dispersal of ZnPc within the fiber matrix. In the case of ZnTAPc and that of (Ac)LuTAPc functionalized fibers, no fluorescence was observed. This is because ZnTAPc has weak fluorescence and (Ac)LuTAPc does not fluoresce at all even in solution. The powder forms of ZnTAPc and (Ac)LuTAPc as well as ZnPc did not fluorescence possibly due to π-π stacking of the phthalocyanine molecules which quenches fluorescence (in addition to the effects of the amino group) and thus, not emissive (36).

3.3. Optical Detection of Nitrogen Dioxide Gas ($NO_{2(g)}$)

We further established that the functionalities of the phthalocyanines are maintained within the fiber matrices by examining the fluorescence behavior of PAA/ZnPc in the presence of nitrogen dioxide. Nitrogen oxides (NO_x) are among the most toxic gaseous pollutants and are major components of outdoor air pollution which directly affect humans (37). Hence, various attempts have been made to develop methods for detection and quantifying these gases (38, 39). In particular, the concentration of nitrogen dioxide (NO_2) has been found to increase spontaneously on the onset of fire and this is independent of the material involved in the burning (40). Therefore, nitrogen dioxide (NO_2) in the gas phase is an early indicator of heat. In this work, we applied the emissive zinc phthalocyanine/polyacrylic acid (PAA/ZnPc) composite fiber, which is permeable to gases as a nanofabric material for fluorometric detection of NO_2.

We begin our investigation by observing the fluorescence behavior of ZnPc (in solution not in fiber form) in DMF solution in the presence of NO_2. As shown in Figure 10, we observed a decrease of the fluorescence intensity of the ZnPc as the solution is exposed to NO_2 gas generated from a reaction of copper metal and dilute nitric acid. Though we could not quantify the amount of NO_2 at each exposure, the changes in the emission spectra suggest that such a chemical entity would be a promising detector of NO_2.

The PAA/ZnPc fiber mat was exposed to NO_2 gas and fluorescence images recorded. As shown in Figure 11, the emission intensity was observed to rapidly diminish on exposure to NO_2. Though we could not again readily quantify the amount of NO_2 available at any time, the results suggest that the fabric material is gas permeable and a promising detector of the gas in the environment. Other polymer supports for ZnPc such thin films have been reported for the detection of NO_2 (41). However, the use of electrospun nanofabric materials is reported for the first time and

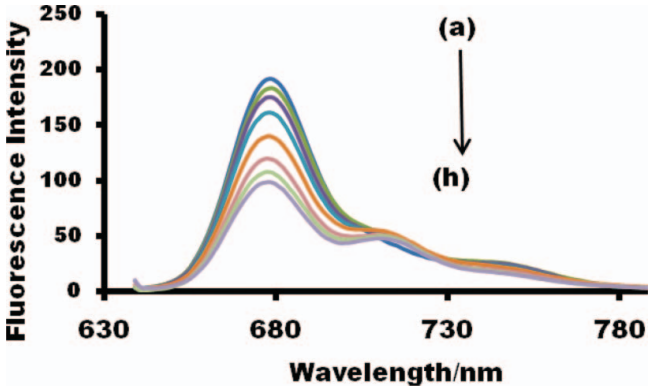

Fig. 10. Decrease in the fluorescence intensity of ZnPc with an introduction of NO_2(g). (Color figure available online).

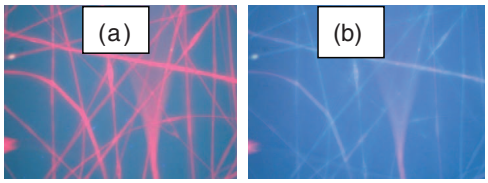

Fig. 11. Detection of NO_2(g) using PAA/ZnPc fiber: Before (a) and after (b) exposure to NO_2 gas. (Color figure available online).

remains much more promising for large scale application due to the ease of production of these nanofabrics.

4 Conclusions

In this work, (Ac)LuTAPc was synthesized and characterized using conventional spectroscopic methods. It was found to be photoactive with triplet quantum yield of 0.43 and lifetime of 3.74 ± 0.01 μs and compared to ZnTAPc with triplet quantum yield of 0.24 and lifetime of 3.32 ± 0.01 μs The singlet oxygen quantum yield in DMF was found to be 0.29 for (Ac)LuTAPc. However, this complex was found not to fluoresce at all. The singlet oxygen generating ability was maintained in the fiber for all the conjugates. The polymeric fiber incorporating unsubstituteded zinc phthalocyanine was further found to be a promising material for the detection of nitrogen dioxide by fluorescence quenching.

Acknowledgments

This work was supported by the Department of Science and Technology (DST) and National Research Foundation (NRF) of South Africa through DST/NRF South African Research Chairs Initiative for Professor of Medicinal Chemistry and Nanotechnology and Rhodes University.

References

1. Kasuga, K. and Tsutsui, M. (1980) *Coord. Chem. Rev.*, 32, 67–95.
2. Honeybourne, C.L. (1987) *J. Phys. Chem. Solids*, 48, 109–141.
3. Colins, R.A. and Mohammed, K.A. (1988) *J. Phys, D.*, 21, 154–161.
4. Bonnett, R. In, *Chemical Aspects of Photodynamic Therapy*; Gordon and Breach Science: Amsteldijk, The Netherlands, 199–222, 2000.
5. Kaestner, L., Cesson, M., Kassab, K., Christensen, T., Edminson, P.D., Cook, M.J., Chambrier, I., and Jori, G. (2003) *Photochem. Photobiol. Sci.*, 2, 660–667.
6. Hassan, S.A., Yehia, F.Z., Hassan, H.A., Sadek S.A., and Darwish, A.S. (2010) *J. Mol. Cat. A: Chem.*, 332, 93–105.
7. Montforts, F.P., Gerlach, B., and Hoper, F. (1994) *Chem. Rev.*, 94, 327–349.
8. Mosinger, J., Lang, K., Kubát, P., Sýkora, J., Hof, M., Plíštil, L., and Mosinger, B., Jr. (2009) *J. Fluoresc.*, 19, 705–713.
9. Tsuiki, H. and Masuda, E. (1996) *Polymer.*, 37, 3637–3644.
10. Shirai, H., Higaki, S., Hanabusa, K., Kondo, Y., and Hojo, N. (1984) *J. Polym. Sci. Polym. Chem. Ed.*, 22, 309–1316.
11. Frenot, A. and Chronakis, I.S. (2003) *Curr. Opin. Colloid Interface Sci.*, 8, 64–75.
12. Li, D. and Xia, Y.N. (2004) *Adv. Mater.*, 16, 1151–1170.
13. Tang, S., Shao, C., Liu, Y., Li, S., Mu, R. (2007) *J. Phys. Chem. Solids.*, 68, 2337–2340.
14. McNamara, C.A., Dixon, M.J., and Bradley, M. (2002) *Chem. Rev.*, 10, 3275–3300.
15. Young, J.G. and Onyebuagu, W. (1990) *J. Org. Chem.*, 55, 2155–2159.
16. Britton. J., Antunes, E., and Nyokong, T. (2010) *J. Photochem. Photobiol. A. Chem.*, 210, 1–7.
17. Achar, B.N., Fohlen, G.M., Parker, J.A., Keshavayya, J. (1987) *Polyhedron*, 6, 1463–1467.
18. Kubát, P. and Mosinger, J. (1996) *J. Photochem. Photobiol. A: Chem.*, 96, 93–97.
19. Kossanyi, J. and Chachraoui, D. (2000) *Int. J. Photoenergy*, 2, 9–15.
20. Fery-Forgues, S., Lavabre, D. (1999) *J. Chem. Ed.*, 76, 1260–1264.
21. Shen, T., Yuan, Z.-I., and Xu, H.-J. (1989) *Dyes Pigm.*, 11, 77–80.
22. Zhang, X.-F., Li, X., Niu, L., Sun, L., and Liu, L. (2009) *J. Fluoresc.*, 19, 947–954.
23. Zhang, X.-F., and Xu, H.-J. (1993) *J. Chem. Soc. Faraday Trans.*, 89, 3347–3351.
24. Nyokong, T. (2007) *Coord. Chem. Rev.*, 25, 1707–1722.
25. Nyokong, T. and Antunes, E. (2010) In, *The Handbook of Porphyrin Science*, Kadish, K.M.; Smith, K. M.; Guilard, R. (Eds.) Academic Press: New York, Vol. 7, Chapt. 34, pp. 247–349, World Scientific: Singapore.
26. Ogunsipe, A., Maree, D. and Nyokong, T. (2003) *Mol. Struct.*, 650, 131–140.
27. Silverstein, R.M., Bassler, G.C., and Morrill, T.C. (1981) *Spectrometric Identification of Organic Compounds*, 4th Ed. John Wiley and Sons: New York.
28. Zugle, R., Litwinski, C., and Nyokong, T. (2011) *Polyhedron*, 30, 1612–1619.
29. Darwent, J.R., Douglas, P., Harriman, A., Porter, G., and Richoux, M.C. (1982) *Coord. Chem. Rev.*, 44, 83–126.
30. Gürol, I., Durmuş, M., Ahsen, V., and Nyokong, T. (2007) *Dalton Trans*., 3782–3791.
31. Fong, H., Chun, I., and Reneker, D.H. (1999) *Polymer*, 40, 4585–4592
32. Triggs, N.E., and Valentini, J.J. (1992) *J. Phys. Chem.*, 96, 6922–6931.
33. Gani, D., Hendra, P.J., Maddams, W.F., Passingham, C., Royaud, I.A.M., Willis, H.A., Zichy, V., and Cudby, M.E.A. (1990) *Analyst*., 115, 1313–1318.
34. Achar, B.N. and Lokesh, K.S. (2004) *J. Organomet. Chem.*, 689, 2601–2605.
35. Lang, K., Mosinger, J., and Wagnerová, D.M. (2004) *Coord. Chem. Rev.*, 248, 321–350.
36. Ngai, T., Zhang, G., Li, X., Ng, D.K.P., and Wu, C. (2001) *Langmuir*, 17, 1381–1383.
37. Capone, S., Rella, R., Siciliano, P., and Vasanelli, L. (1999) *Thin Solid Films*, 350, 264–268.
38. Fontijin, A., Sabadell, A. J., and Ronco R. (1970) *J. Anal. Chem.*, 42, 575–579.
39. Maeda, Y., Aoki, K., and Munemori, M. (1980) *Anal. Chem.*, 52, 307–311.
40. Nezel, T., Spichiger-Keller, U.E., Ludin, C., and Hensel, A. (2001) *Chimia*, 55, 725–731
41. Inagaki, N., Tasaka, S., and Sei, Y. (1996) *Polym. Bull.*, 36, 601–607.